



Contents lists available at ScienceDirect

Journal of Biomechanics

journal homepage: www.elsevier.com/locate/jbiomech
www.JBiomech.com

Short communication

Influence of IMU position and orientation placement errors on ground reaction force estimation [☆]Tian Tan ^a, David P. Chiasson ^a, Hai Hu ^b, Peter B. Shull ^{a,*}^a State Key Laboratory of Mechanical System and Vibration, School of Mechanical Engineering, Shanghai Jiao Tong University, Shanghai 200240, China^b Department of Orthopaedic Surgery, Shanghai Jiao Tong University, Affiliated Sixth People's Hospital, Shanghai 200233, China

ARTICLE INFO

Article history:

Accepted 6 October 2019

Keywords:

Ground reaction force
Position error
Orientation error

ABSTRACT

Wearable inertial measurement units (IMU) have been proposed to estimate GRF outside of specialized laboratories, however the precise influence of sensor placement error on accuracy is unknown. We investigated the influence of IMU position and orientation placement errors on GRF estimation accuracy. Methods: Kinematic data from twelve healthy subjects based on marker trajectories were used to simulate 1848 combinations of sensor position placement errors (range ± 100 mm) and orientation placement errors (range $\pm 25^\circ$) across eight body segments (trunk, pelvis, left/right thighs, left/right shanks, and left/right feet) during normal walking trials for baseline cases when a single sensor was misplaced and for the extreme cases when all sensors were simultaneously misplaced. Three machine learning algorithms were used to estimate GRF for each placement error condition and compared with the no placement error condition to evaluate performance. Results: Position placement errors for a single misplaced IMU reduced vertical GRF (VGFR), medio-lateral GRF (MLGRF), and anterior-posterior GRF (APGRF) estimation accuracy by up to 1.1%, 2.0%, and 0.9%, respectively and for all eight simultaneously misplaced IMUs by up to 4.9%, 6.0%, and 4.3%, respectively. Orientation placement errors for a single misplaced IMU reduced VGFR, MLGRF, and APGRF estimation accuracy by up to 4.8%, 7.3%, and 1.5%, respectively and for all eight simultaneously misplaced IMUs by up to 20.8%, 23.4%, and 12.3%, respectively. Conclusion: IMU sensor misplacement, particularly orientation placement errors, can significantly reduce GRF estimation accuracy and thus measures should be taken to account for placement errors in implementations of GRF estimation via wearable IMUs.

© 2019 Elsevier Ltd. All rights reserved.

1. Introduction

Ground reaction force (GRF) measurement is critical for gait assessment and intervention. In contrast with the traditional approach of measuring GRF via floor-mounted force plates inside of specialized laboratories, GRF estimation via wearable sensors such as inertial measurement units (IMUs) could enable daily life disease monitoring and assessment such as Parkinson's disease

monitoring (Aşuroğlu et al., 2018), walking balance assessment after stroke (Van Meulen et al., 2016), and gait symmetry monitoring after total knee arthroplasty (Christensen et al., 2018). Researchers have attempted to combine a dynamic human model with kinematic data measured by different amount of IMUs to estimate GRF. Yang and Mao (Yang and Mao, 2015) used a 3D analytical model with seven IMUs to estimate GRF magnitudes during walking, and the root mean square error (RMSE) of GRF magnitude estimation varied between 44 N and 66 N. Karatsidis et al. (2016) used a 16-segment human model and 17 IMUs to predict 3-axis GRF during walking. The normalized root mean square error (NRMSE) of vertical GRF (VGFR), medio-lateral GRF (MLGRF), and anterior-posterior GRF (APGRF) were 5.3%, 12.4%, and 9.4%. Apart from human-model-based methods, attempts to estimate GRF using machine learning algorithms also achieved promising results. Leporace et al. (2015) used a three-layer Artificial Neural Network (ANN) and one accelerometer attached to the shank to estimate 3-axis GRF during walking. The normalized mean absolute deviation of VGFR, MLGRF, and APGRF were 4.7%, 12.8%, and

[☆] All authors have made substantial contributions to the following: (1) the conception and design of the study, or acquisition of data, or analysis and interpretation of data, (2) drafting the article or revising it critically for important intellectual content, (3) final approval of the version to be submitted. Each of the authors has read and concurs with the content in the manuscript. The manuscript and the material within have not been and will not be submitted for publication elsewhere.

* Corresponding author at: Room 930, Mechanical Engineering Bld. A, School of Mechanical Engineering, Shanghai Jiao Tong University, 800 Dong Chuan Road, Shanghai 200240, China.

E-mail address: pshull@sjtu.edu.cn (P.B. Shull).

5.2% respectively. Guo et al. (2017) used an orthogonal forward regression algorithm and acceleration data obtained from three IMUs to estimate the vertical GRF during walking, and the mean NRMSE was less than 5.0%. Wouda et al. (2018) used a four-layer ANN and three IMUs placed on the pelvis and both shanks to estimate the vertical GRF during running, and the mean RMSE was lower than 0.27 N/BW.

One major potential problem with an IMU system is that its performance can be reduced by the placement error. A study of four critical sources of error across the IMU system showed that the placement error is the biggest challenge compared with manufacturing variations and environmental conditions, IMU synchronization, and integration drift (Chen et al., 2013). Some IMU based activity recognition studies showed that the position placement error, orientation placement error, and their combinations would result in significant recognition rate decrease (Banos et al., 2014; Kunze and Lukowicz, 2014; Yurtman and Barshan, 2017). Similarly, without proper calibration procedure, considerable accuracy degradation can be observed when measuring gait parameters such as joint angle (Vargas-Valencia et al., 2016) and stride length (Chen et al., 2014). The precision of IMU placement is important when using machine learning algorithms because the estimation models learn the relationship between the input and output based on the training data. However, even if the subject's gait was identical during testing, the incorrect IMU placement would affect the magnitude and direction of the measured acceleration and angular velocity, which might make the estimation result unreliable. Though there is a general understanding that the GRF estimation accuracy can be reduced by placement error, its effect, to the best of our knowledge, has not been systematically investigated. The purpose of this paper was to systematically investigate the influence of single and multiple simultaneous IMU position and orientation placement errors on GRF estimation accuracy. This work is the first to directly compare the influence of position placement errors versus orientation placement errors on GRF estimation accuracy across trunk, pelvis, both thighs, both shanks, and both feet.

We hypothesized that the orientation placement error would result in a larger accuracy decrease than position placement error because the orientation placement error would negatively influence both accelerometer and gyroscope data while the position placement error would not affect gyroscope data.

2. Methods

2.1. GRF estimation

Three standard machine learning algorithms were used to evaluate the influence of sensor placement errors on GRF accuracy: Support Vector Regression (SVR), Gradient Boosting Decision Tree (GBDT), and Artificial Neural Network (ANN). For SVR, the kernel was a radial basis function, its coefficient was 0.01, and the penalty parameter was 10. For GBDT, the number of boosting stages to perform was 500, the learning rate was 0.1, and the maximum depth of the decision tree was 6. For ANN, apart from the input and output layer, there were two hidden layers which had 40 and 8 neurons. The activation function of the hidden layer and output layer were rectified linear unit function and identity function, respectively. All three machine learning algorithms were implemented and trained using the Python Scikit-learn library (Fabian et al., 2011).

Previous research showed that IMU can be re-simulated from known segment trajectory and orientation data (Young et al., 2011). In this paper, we obtained the human body segment trajectory and orientation from marker data, obtained simulated accelerometer data from segment trajectory, and obtained simulated gyroscope data from segment orientation (see Supplementary Material I for IMU simulation details). IMU data were simulated at 100 Hz from a freely available walking gait marker data set (Moore et al., 2015) at the following locations (Fig. 1): 7th cervical vertebrae (trunk), middle of left and right posterior superior iliac spines (pelvis), middle of greater trochanter and lateral epicondyle of the knee (left/right thighs), middle of lateral epi-

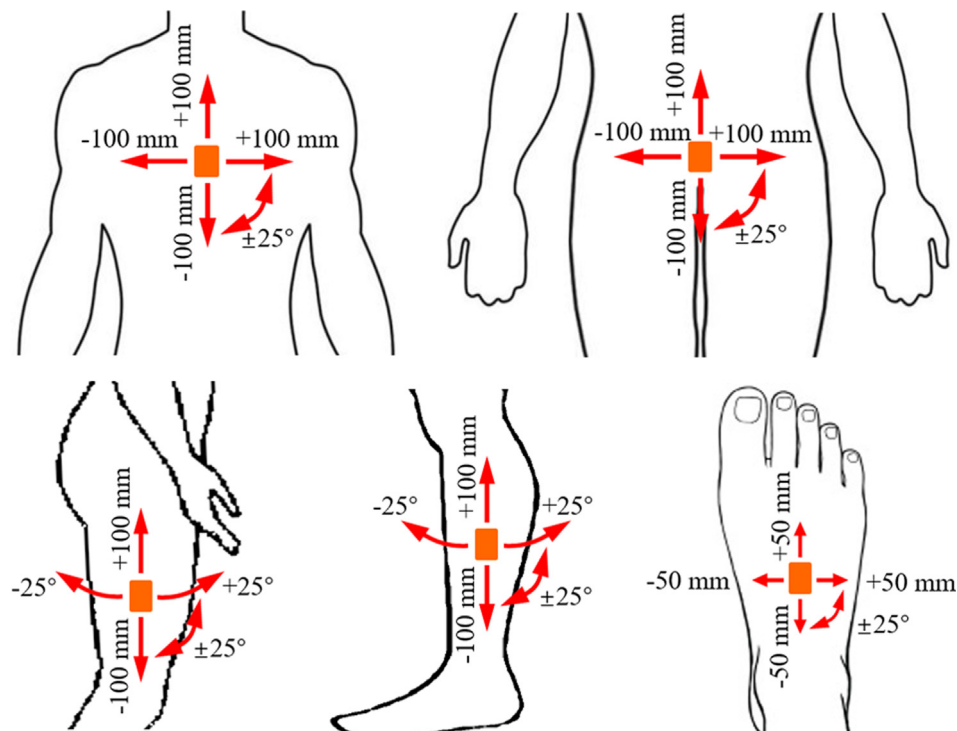


Fig. 1. Simulated IMU placement errors from the original IMU positions at the trunk, pelvis, both thighs, both shanks, and both feet.

condyle of the knee and lateral malleolus of the ankle (left/right shanks), and middle of heel and toe (left/right feet). GRF was measured by an R-Mill treadmill which has dual 6 degrees of freedom force plates. The GRF was sampled at 100 Hz, synchronized with simulated IMU data, and low-pass filtered at 25 Hz using a zero-lag, fourth-order Butterworth filter. Forty-eight input features (3-axis acceleration and 3-axis angular velocity of above-mentioned eight simulated IMUs) were used to estimate VGRF, MLGRF, and APGRF of the left foot. The GRF measured by the force plates was used as the output in model training and was used as the true value to evaluate the estimation accuracy in model testing. GRF was normalized by subject weight. Leave-one-out cross-validation was used to evaluate performance. For the training and testing data, each input feature was normalized by removing the mean and scaling to unit variance.

2.2. Quantifying influence of IMU placement errors

We investigated the influence of baseline cases when a single IMU was misplaced and extreme cases when all IMUs were simultaneously misplaced from walking data of twelve young subjects walking at three speeds (0.8, 1.2, and 1.6 m/s) on an instrumented treadmill from a freely available walking gait marker data set (Moore et al., 2015). For both cases, position errors, orientation errors, and position + orientation errors were investigated, and thus the six types of placement errors were (see Supplementary Material II for placement error details): (1) Single IMU position errors, (2) Single IMU orientation errors, (3) Single IMU position + orientation errors, (4) All IMU simultaneous position errors, (5) All IMU simultaneous orientation errors, and (6) All IMU simultaneous position + orientation errors. The position placement errors were generated by moving the simulated IMU from its original location to a new attachment location. The IMU moves on the body segment, with the bottom of the IMU always tangentially attached to the surface and the z-axis of the IMU aligned with the surface normal. The orientation placement errors were generated by applying a rotation matrix to the IMU data. The IMU rotates along its z-axis while the position of the IMU center remained unchanged. Details about placement error range, direction, and the number of simulated placement errors are described in Supplementary Material II. GRF estimation models were trained using placement-error-free IMU data and were tested using IMU data with each type of placement error. Error ranges (± 100 mm and $\pm 25^\circ$) were determined based on conservative estimates of the maximum human placement errors from pilot testing. We used peak-to-peak normalized root mean square error (NRMSE) to quantify the accuracy decrease, which is defined by:

$$NRMSE = \frac{\sqrt{\frac{\sum_{t=0}^{t_{end}} [(GRF_{j,measured}(t) - GRF_{j,estimated}(t))^2] / N}{\max(GRF_{j,measured}(t)) - \min(GRF_{j,measured}(t))}}}{\max(GRF_{j,measured}(t)) - \min(GRF_{j,measured}(t))} \times 100\%, \quad (1)$$

where t is the time vector with N samples and j is the GRF axis. Due to limited space, results of the worst accuracy degradation of each type of placement error are reported in the paper, and a detailed comparison of GRF estimation accuracy to placement error amount and location is reported in Supplementary Material III.

3. Results

Single IMU placement errors for VGRF reduced accuracy from position placement error by up to 1.0%, from orientation error by up to 3.2%, and from position + orientation errors by up to 3.4% (Fig. 2). All IMU simultaneous placement errors for VGRF reduced accuracy from position placement error by up to 4.4%, from orientation error by up to 11.8%, and from position + orientation errors

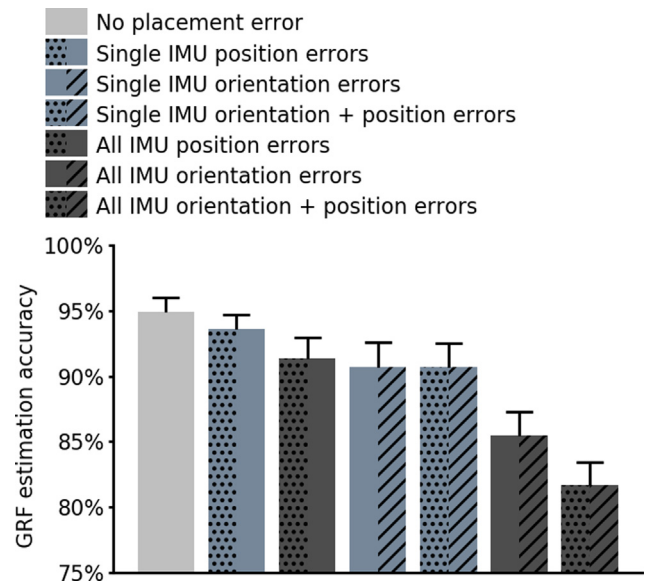


Fig. 2. Representative VGRF estimation accuracy decrease due to single and all IMU position, orientation, and position + orientation placement errors at a 1.2 m/s walking speed using the ANN algorithm. Bar height was 100% - NRMSE (1 standard deviation) of that type of placement errors. Light gray bars represent single IMU placement errors; dark gray bars represent all IMU placement errors. Dots on the left side of the bar represent position errors; slashes on the right side of the bar represent orientation errors.

by up to 17.1% (Fig. 2). Similarly, the accuracy degradation caused by orientation errors was equal to or higher than that of position errors for all three GRF axes and all three walking speeds (Table 1).

Comparing the results between GRF axes, the NRMSE of MLGRF was the highest and the NRMSE of APGRF was slightly lower than VGRF (Table 1). Additionally, for single IMU position and single IMU orientation errors, the influence of orientation placement error of trunk IMU was substantially higher than all other IMUs for all three algorithms (Fig. 3). For single IMU position errors, no substantial difference was observed between IMUs of different segments. For both types of placement errors, the NRMSE of GBDT and ANN based model was similar to each other and was lower than the SVR based model.

4. Discussion

This work systematically investigated the influence of single and multi-segment IMU simultaneous position and orientation placement errors on the accuracy of GRF estimation. We used 12 subjects' body segment marker trajectories during normal walking to simulate IMU data across eight body segments. SVR, GBDT, and ANN standard machine learning algorithms were used to generate GRF estimation models and resulting accuracies were compared. For both single and multi-segment IMU placement errors, the orientation placement errors had a higher influence on estimation accuracy than position placement errors, which corroborates the conclusion provided by Miezal et al. (2016). The NRMSE difference between single IMU orientation errors and single IMU position + orientation errors was relatively small, suggesting that orientation error was the major contributor to the reduced accuracy of single IMU position + orientation error condition. One possible explanation for the higher impact of orientation errors is that the orientation placement error would have had a negative effect on both accelerometer and gyroscope data, while the position placement error wouldn't affect gyroscope data.

Table 1
Vertical, medio-lateral, and anterior-posterior ground reaction force errors at three walking speeds. Errors were reported as Maximum NRMSE (1 standard deviation). The machine learning algorithm was ANN.

Walking speed	GRF component	No placement error (%)	Single IMU placement errors (%)			All IMU placement errors (%)		
			Position	Orientation	Position + orientation	Position	Orientation	Position + orientation
0.8 m/s	VGRF	6.3 (3.0)	7.4 (3.0)	11.1 (3.5)	11.2 (3.4)	9.9 (3.5)	27.1 (5.8)	32.4 (6.5)
	MLGRF	8.6 (1.6)	10.7 (2.1)	16.3 (5.9)	16.6 (5.9)	13.5 (2.8)	32.1 (11.7)	37.3 (13.2)
	APGRF	5.7 (1.6)	6.6 (1.3)	7.3 (1.2)	8.2 (2.0)	9.7 (1.8)	18.0 (2.7)	17.3 (2.9)
1.2 m/s	VGRF	4.9 (1.2)	5.9 (2.0)	8.2 (1.9)	8.3 (1.8)	9.3 (2.7)	20.0 (4.3)	25.3 (5.0)
	MLGRF	7.5 (1.1)	9.1 (1.2)	11.2 (3.2)	11.5 (3.1)	13.2 (2.0)	20.9 (7.6)	28.2 (9.1)
	APGRF	4.3 (1.2)	5.1 (0.9)	5.3 (1.2)	6.2 (1.2)	8.6 (1.0)	10.9 (1.9)	12.4 (1.7)
1.6 m/s	VGRF	5.1 (1.9)	6.1 (2.3)	7.5 (1.7)	7.6 (1.8)	10.0 (2.9)	16.1 (3.3)	19.3 (4.2)
	MLGRF	7.8 (2.3)	9.6 (2.1)	9.9 (3.0)	10.6 (3.2)	13.8 (2.8)	16.9 (5.4)	24.9 (6.9)
	APGRF	3.7 (1.0)	4.6 (0.6)	4.5 (0.8)	5.1 (0.9)	7.8 (1.0)	8.6 (1.4)	11.2 (1.2)

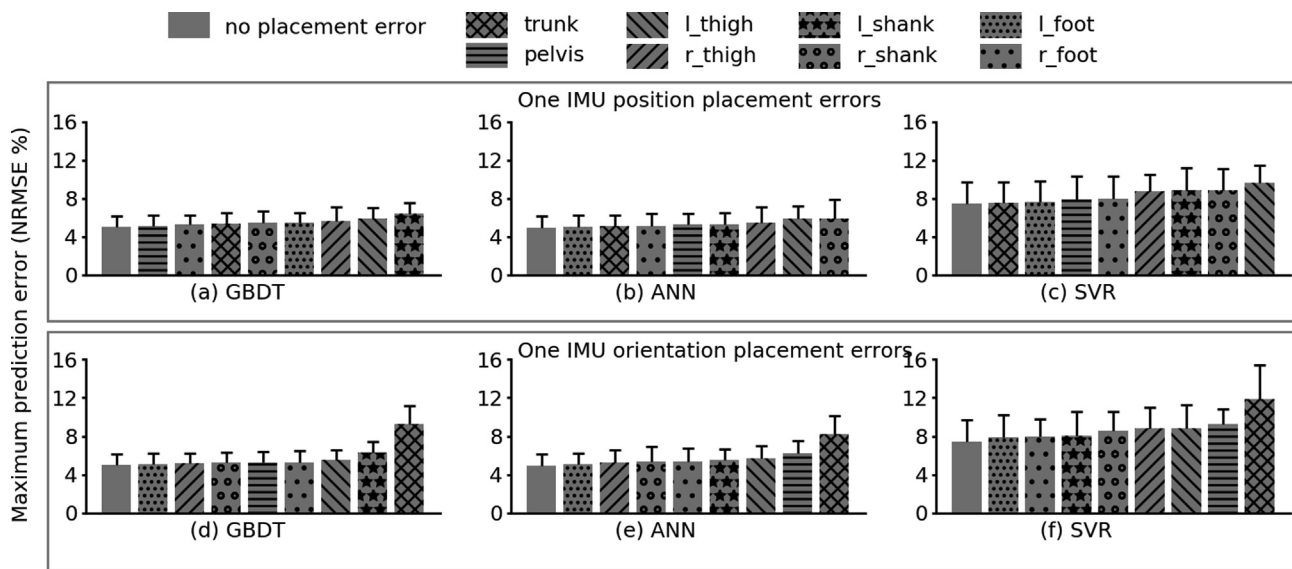


Fig. 3. Representative comparison of the influence of different segment IMUs and different machine learning algorithms for VGRF at a walking speed of 1.2 m/s. The algorithms were GBDT for (a) and (d), ANN for (b) and (e), and SVR for (c) and (f). For each segment IMU, the corresponding bar represents the maximum NRMSE among all the simulated position placement errors (a)–(c), and orientation placement errors (d)–(f).

Although orientation placement errors resulted in larger accuracy decrease, such a decrease can be alleviated if the model inputs are orientation-invariant features. These kind of features can be obtained by calculating the magnitude of acceleration and angular velocity, or by transformations such as Singular Value Decomposition (Yurtman and Barshan, 2017). Also, orientation placement errors can potentially be corrected by rotating the measured data from IMU frame to segment frame using IMU-to-segment orientation acquired by static calibration (Roetenberg et al., 2009), functional calibration (Ligorio et al., 2017), self-calibration (Taetz et al., 2016), or deep learning algorithm based calibration (Zimmermann et al., 2018).

Comparing results between algorithms, though the overall accuracy of SVR based model was lower than that of GBDT and ANN, consistency can be found in three algorithms' sensitivity to placement errors, indicating that the placement error impacts concluded in this paper are likely to be applicable to other GRF estimation algorithms using machine learning. For example, for all three algorithms, the trunk IMU's orientation errors had a significantly higher impact than other segment IMUs while no obvious difference can be found between position errors of eight IMUs (Fig. 3). One possible reason for the lower accuracy of SVR based models is that GBDT and ANN use least squares as the loss function where the root mean square error is minimized, while SVR uses an epsilon-intensive loss function where the absolute distance

between the observed output and the boundary is minimized (Jap et al., 1997).

Among the three GRF axes, the NRMSE of MLGRF was the highest, likely because its amplitude was significantly lower than that of the other two axes during walking. This finding is also consistent with other GRF estimation results obtained using direct human modeling (Karatsidis et al., 2016), simple linear models (Shahabpoor et al., 2018), and ANN (Leporace et al., 2015). The NRMSE of APGRF was slightly lower than that of VGRF, which is similar to the result obtained in Leporace et al., 2015, possibly due to the similarity of the proposed models.

It is important to note that the results presented in the paper and Supplementary Material III apply specifically to the placement errors simulated in this experiment. The accuracy degradation would be different if the amount, direction, or combinations of placement errors were different.

In conclusion, the accuracy of GRF estimation is more likely to be adversely affected by orientation placement errors than by position placement errors. Additionally, correct orientation placement of the trunk IMU is more important than the orientation placement of the IMUs located at the pelvis or lower extremities. When researchers and therapists use IMUs to estimate GRF for outdoor gait monitoring and disease assessment, they should carefully perform IMU (especially trunk IMU) orientation placement. Correction methods such as static calibration (Roetenberg et al., 2009) or

functional calibration (Ligorio et al., 2017) could also be considered to reduce the influence of placement error.

Declaration of Competing Interest

None of the authors had any conflict of interest regarding this manuscript.

Acknowledgments

This work was supported by the National Natural Science Foundation of China (51875347 and 31270996).

Appendix A. Supplementary material

Supplementary data to this article can be found online at <https://doi.org/10.1016/j.jbiomech.2019.109416>.

References

- Aşuroğlu, T., Açıcı, K., Berke Erdaş, Ç., Kılınc Toprak, M., Erdem, H., Oğul, H., 2018. Parkinson's disease monitoring from gait analysis via foot-worn sensors. *Biocybern. Biomed. Eng.* 38, 760–772.
- Banos, O., Toth, M.A., Damas, M., Pomares, H., Rojas, I., 2014. Dealing with the effects of sensor displacement in wearable activity recognition. *Sensors* 14, 9995–10023.
- Chen, S., Brantley, J.S., Kim, T., Ridenour, S.A., Lach, J., 2013. Characterising and minimising sources of error in inertial body sensor networks. *Int. J. Auton. Adapt. Commun. Syst.* 6, 253.
- Chen, Y., Hu, W., Yang, Y., Hou, J., Wang, Z., 2014. A method to calibrate installation orientation errors of inertial sensors for gait analysis. In: 2014 IEEE Int Conf. Inf. Autom. ICIA, pp. 598–603.
- Christensen, J.C., Foreman, K.B., LaStayo, P.C., Marcus, R.L., Pelt, C.E., Mizner, R.L., 2018. Comparison of 2 forms of kinetic biofeedback on the immediate correction of knee extensor moment asymmetry following total knee arthroplasty during decline walking. *J. Orthop. Sport. Phys. Ther.* 49 (2), 105–111.
- Fabian, Pedregosa, Michel, V., Grisel, Olivier, Blondel, M., Prettenhofer, P., Weiss, R., Vanderplas, J., Cournapeau, D., Pedregosa, F., Varoquaux, G., Gramfort, A., Thirion, B., Grisel, O., Dubourg, V., Passos, A., Brucher, M., Perrot, M., Duchesnay, É., 2011. Scikit-learn: machine learning in python. *J. Mach. Learn. Res.* 12, 2825–2830.
- Jap, D., Stöttinger, M., Bhasin, S., 1997. Support vector regression machines. *Adv. Neural Inf. Process. Syst.*, 155–161.
- Karatsidis, A., Bellusci, G., Schepers, H., de Zee, M., Andersen, M., Veltink, P., 2016. Estimation of ground reaction forces and moments during gait using only inertial motion capture. *Sensors* 17, 75.
- Kunze, K., Lukowicz, P., 2014. Sensor placement variations in wearable activity recognition. *IEEE Pervasive Comput.* 13, 32–41.
- Leporace, G., Batista, L.A., Metsavaht, L., Nadal, J., 2015. Residual analysis of ground reaction forces simulation during gait using neural networks with different configurations. *Conf. Proc. IEEE Eng. Med. Biol. Soc.* 2015, 2812–2815.
- Ligorio, G., Zanotto, D., Sabatini, A.M., Agrawal, S.K., 2017. A novel functional calibration method for real-time elbow joint angles estimation with magnetic-inertial sensors. *J. Biomech.* 54, 106–110.
- Miezel, M., Taetz, B., Bleser, G., 2016. On inertial body tracking in the presence of model calibration errors. *Sensors* 16, 1–34.
- Moore, J.K., Hnat, S.K., van den Bogert, A.J., 2015. An elaborate data set on human gait and the effect of mechanical perturbations. *PeerJ* 3, e918.
- Roetenberg, D., Luinge, H., Slycke, P.J., 2009. Xsens MVN: Full 6DOF human motion tracking using miniature inertial sensors. *XSENS Technol.*, 1–9.
- Shahabpoor, E., Pavic, A., Brownjohn, J.M.W., Billings, S.A., Guo, L., Bocian, M., 2018. Real-life measurement of tri-axial walking ground reaction forces using optimal network of wearable inertial measurement units. *IEEE Trans. Neural Syst. Rehabil. Eng.* 26, 1–10.
- Taetz, B., Bleser, G., Miezel, M., 2016. Towards self-calibrating inertial body motion capture. In: 19th International Conference on Information Fusion, pp. 1751–1759.
- Van Meulen, F.B., Weenk, D., Buurke, J.H., Van Beijnum, B.J.F., Veltink, P.H., 2016. Ambulatory assessment of walking balance after stroke using instrumented shoes. *J. Neuroeng. Rehabil.* 13, 1–10.
- Vargas-Valencia, L.S., Elias, A., Rocon, E., Bastos-Filho, T., Frizera, A., 2016. An IMU-to-body alignment method applied to human gait analysis. *Sensors* 16, 1–17.
- Young, A.D., Ling, M.J., Arvind, D.K., 2011. IMUSim: A simulation environment for inertial sensing algorithm design and evaluation. In: Proc. 10th ACM/IEEE Int. Conf. Inf. Process. Sens. Networks, pp. 199–210.
- Yurtman, A., Barshan, B., 2017. Activity recognition invariant to sensor orientation with wearable motion sensors. *Sensors* 17, 1838.
- Zimmermann, T., Taetz, B., Bleser, G., 2018. IMU-to-segment assignment and orientation alignment for the lower body using deep learning. *Sensors* 18, 1–35.